Surface plasmonic lattice solitons

Yao Kou, Fangwei Ye,* and Xianfeng Chen

Department of Physics, The State Key Laboratory on Fiber Optic Local Area Communication Networks and Advanced Optical Communication Systems, Shanghai Jiao Tong University, Shanghai 200240, China

**Corresponding author: fangweiye@sjtu.edu.cn*

Received June 11, 2012; accepted August 2, 2012;
posted August 6, 2012 (Doc. ID 170207); published September 11, 2012

We reveal the existence of the surface plasmonic lattice solitons (surface PLSs) at the boundary of a semi-infinite metallic-dielectric periodic nanostructure. We find that the truncation of the periodic structure imposes a threshold power for the existence of surface PLSs, and significantly enhances the modal localization. The propagation and excitation of surface PLSs as well as their potential application in the all-optical subwavelength switching are also demonstrated.

OCIS codes: 190.6135, 190.4360, 240.6680.

Light interaction with photonic periodic lattice has been studied extensively because of its fundamental and practical importance [1]. The study of such interaction in the presence of nonlinear optical response has drawn great attention as the nonlinearity affords light-controlled tunability [2,3]. Discrete solitons [4,5], or more generally lattice solitons, are one of the most exciting outcomes of such nonlinear interaction, and they were investigated in perfect lattice and various inhomogeneous lattice structures. Especially worthy to be mentioned is the so-called surface lattice solitons occurring at the boundary of a truncated lattice [6–8], which differ profoundly from their counterpart in homogenous lattices. So far, however, surface lattice solitons are all studied at the edge of *dielectric* waveguides.

There is increasing interest in pushing the study of nonlinear light-lattice interaction into the subwavelength region, where the conventional dielectric lattice is replaced by a plasmonic lattice [9–12]. Plasmonic lattice is composed of alternative nanoscale metallic and dielectric materials. Tunneling of surface plasmonic polaritons (SPPs) between adjacent metallic components in plasmonic lattices might be inhibited by the nonlinearity of the dielectric medium, leading to the formation of so-called plasmonic lattice solitons (PLSs) [10]. In this Letter, we truncate the plasmonic lattice and consider the influence of the resulting lattice boundary on PLSs. We reveal the existence of a new type of nonlinear surface states, that is, surface PLSs. The properties of surface PLSs are crucially determined by the boundary effect. This includes the occurrence of a threshold power for their formation and the double-enhanced modal localization in comparison with their PLS counterparts. The propagation and excitation of surface PLSs are studied in detail, and their potential application in all-optical switching at the deep-subwavelength scale is also presented.

We thus consider the wave propagation along the interface between a uniform media ($x < 0$) and a one-dimensional nonlinear plasmonic lattice ($x > 0$). Without loss of generality, unless otherwise stated, the width of metal and Kerr-type nonlinear dielectric layers are fixed as $t_m = 60$ nm and $t_d = 100$ nm, respectively. The refractive index of the nonlinear layers is assumed to be intensity-dependent as $n_{\mathrm{NL}} = \sqrt{\varepsilon_{\mathrm{NL}}} = 1.5 + n_2 I$, where $n_2 = \pm 1.8 \times 10^{-17}$ m^2/W is the Kerr coefficient and the positive (negative) sign represents self-focusing (self-defocusing) nonlinearity, respectively. Intensity $I = (1/2)\varepsilon_0 c n_0 |E|^2$. The complex permittivity of the metal (silver) ε_m is taken from Johnson and Christy [13], which is $\varepsilon_m = -129 + 3.28i$ for the wavelength of $\lambda = 1550$ nm. Finally, the uniform region is assumed to be linear with a permittivity $\varepsilon_d = 2.25$. The results do not change visibly if the intensity-dependent permittivity is also included in this region.

To describe nonlinear stationary modes localized at the surface of the lattice, we consider TM waves ($E_y = H_x = H_z = 0$) with the stationary form:

$$E_x(x, z, t) = [u_x(x)\hat{x}]e^{i(\beta z - \omega t)}, \tag{1}$$

$$H_y(x, z, t) = [v_y(x)\hat{y}]e^{i(\beta z - \omega t)}, \tag{2}$$

where u_x and v_y represent a modal profile independent of z (z is the propagation direction), with β being the soliton propagation constant. Substituting Eqs. (1) and (2) into Maxwell's equations yields the following equations [9]:

$$\frac{k_0 \varepsilon}{z_0} u_x = \beta v_y, \tag{3}$$

$$\frac{z_0}{k_0}\left[\frac{d}{dx}\left(\frac{1}{\varepsilon}\frac{d}{dx}\right) + k_0^2\right] v_y = \beta u_x, \tag{4}$$

where $z_0 = \sqrt{\mu_0/\varepsilon_0}$ is the vacuum impedance, ε denotes the material permittivity as a function of x, and $k_0 = 2\pi/\lambda$. The soliton solutions were numerically found by a self-consistent method [14]. For simplicity, the solutions given below are found without taking into account the metallic loss. We confirmed, however, that inclusion of loss does not change the results significantly.

Surface PLSs are found to be centered their peak amplitude in different nonlinear dielectric layers. Figure 1 shows representative profiles whose peak amplitudes reside at the first or the second waveguide (denoted as $m = 1$ and $m = 2$ modes, respectively) under focusing/defocusing Kerr-type nonlinearities. It can be seen that the solitons' amplitudes decay exponentially fast from their peak-amplitude-resided waveguide into both the uniform and the lattice regions. Because of the boundary effect, however, the decay speed of amplitude in the

uniform region is faster than that in the lattice region. Thus, surface PLSs feature asymmetric profiles. Their asymmetry quickly becomes insignificant when their peak amplitude shifts to the deep lattice region. In fact, for nonlinear index change of $\Delta n = 0.05$, surface PLSs of $m = 4$ are visually symmetric already. Note that the appearance of staggered (unstaggered) surface PLSs in the focusing (defocusing) nonlinearity is a consequence of the inverted diffraction relations that is unique to the plasmonic-lattice systems [9,10].

The characteristic power of surface solitons, defined as $P = (1/2)\int \mathrm{Re}(E_x H_y^*)\mathrm{d}x$, is a conserved quantity in the sense that it remains constant during the propagation of surface solitons. Figures 2(a) and 2(b) plot soliton power versus propagation constant β. Notably, surface PLSs feature some critical power P_c, below which no solutions can be found. This property puts a minimum demand on the laser power to excite such surface solitons, which is in sharp contrast to the PLSs in the homogenous plasmonic lattice [10], as the existence of the latter requires no threshold power (i.e., $P_c = 0$). As one expects, the threshold power substantially decreases with the increasing distance of the peak-centered waveguide from the lattice boundary, as the comparisons shown in Figs. 2(a) and 2(b) for mode $m = 1$ and $m = 2$. The influence of metallic width on P_c is also studied [see Fig. 2(c)]. The dramatic increase of P_c with decreasing metallic width is attributed to the strong coupling of SPPs at the opposite surfaces of each of the metallic layers, thus creating the enhanced diffraction, which in turn requires stronger nonlinearity to balance it.

We emphasize that, essentially different from the surface solitons in the truncated pure-dielectric lattice, surface PLSs reported in this Letter are not diffraction limited, and thus their modal extensions could be nanoscale. To quantitatively characterize the degree of modal localization, we plot the fraction of power concentrating in the first waveguide (for $m = 1$ modes) versus the nonlinear index change. This result is shown in Fig. 2(d).

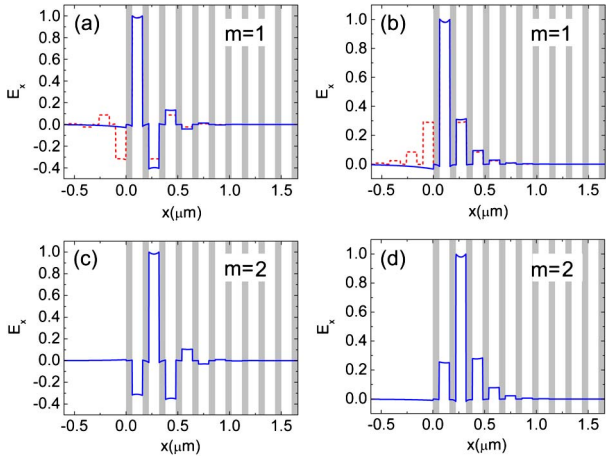

Fig. 1. (Color online) Normalized electric field (E_x) profiles of surface PLSs for the nonlinear index change of (a), (c) $\Delta n = 0.05$; (b), (d) $\Delta n = -0.05$. The gray regions stand for metallic layers, while the white regions for dielectric domains. The red (dashed) lines in (a) and (b) represent the electric field (E_x) profiles of PLSs in the corresponding homogenous plasmonic lattices.

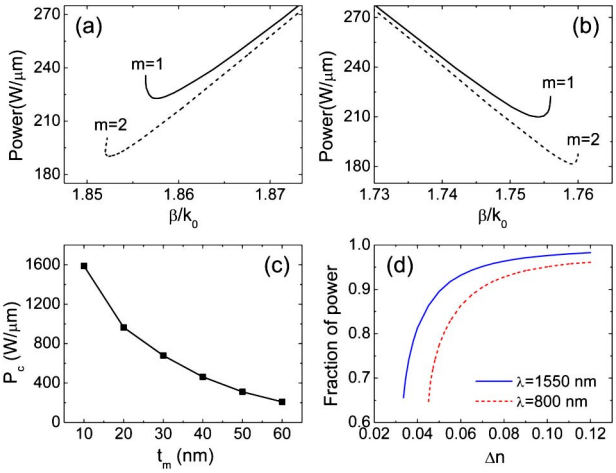

Fig. 2. (Color online) (a), (b) Power versus normalized propagation constants for staggered and unstaggered surface PLSs, respectively. (c) Threshold power P_c of the unstaggered surface PLSs ($m = 1$) as a function of metal layer width t_m. (d) Fraction of power concentrating in the first waveguide versus nonlinear index change Δn, for the unstaggered surface PLSs ($m = 1$).

One sees that for a moderate index change of $\Delta n = 0.05$, more than 90% of the soliton power is confined in the first waveguide, indicating that the transverse size of surface PLSs is less than 0.1λ. Importantly, in the perfect plasmonic lattice, the same amount of index change is found to concentrate mode size of 0.17λ [see Figs. 1(a) and 1(b) for the profiles of solitons in homogenous plasmonic lattices], and thus the energy concentration is almost double enhanced in the presence of lattice boundary. Note that such significant modal compression cannot be achieved by truncating the dielectric lattices, because the surface lattice solitons are limited by diffraction and thus cannot get further compression if the solitons are already at the subwavelength scale. Therefore, the possibility of further significant modal compression by lattice truncation is a unique property of plasmonic lattice, provided that the associated surfaces PLSs exist.

To prove that the above numerically found solutions are indeed stationary eigenmodes of the associated truncated plasmonic lattice, we launch the solutions into the structure and propagate them using finite element method (FEM) software (Comsol Multiphysics). Typical propagation results are shown in Figs. 3(a) and 3(b); indeed, the profiles remain unchanged after a long distance (>100 μm). Moreover, for propagation results shown in Figs. 3(c) and 3(d), the realistic metallic loss is taken into account. From the loss-included mode analysis, for $\lambda = 1550$ nm, surface PLSs have the typical absorption coefficients of ~400 cm^{-1} for staggered solitons and ~250 cm^{-1} for unstaggered solitons, which corresponds to the decay length ~25 μm and ~40 μm, respectively. As clearly seen from Figs. 3(c) and 3(d), even in the lossy case, the soliton propagation is still visible in tens of micrometers.

We finally examine the generation of surface PLSs by means of a single-waveguide excitation setup. In Figs. 4(a) and 4(b), a TM-polarized incident light is launched into the first plasmonic waveguide. Experimentally, such excitation might be achieved by, for example, tapered couplers [15] or dipole nanoantennas [16]. We observe

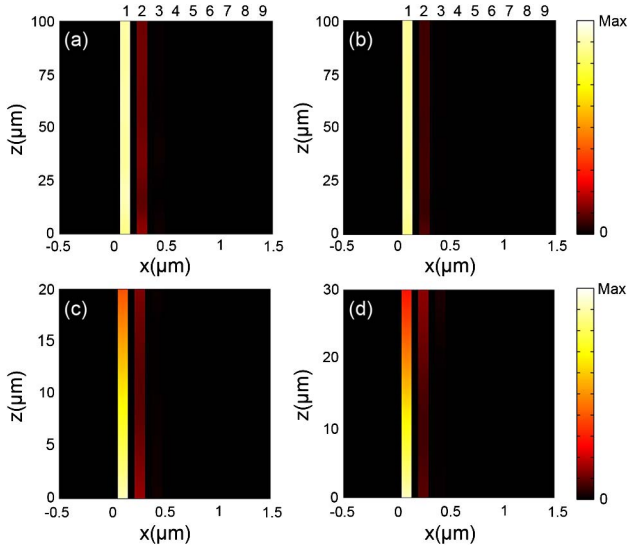

Fig. 3. (Color online) Propagation of (a) staggered surface PLSs, and (b) unstaggered surface PLSs in the lossless plasmonic lattices, corresponding to $\Delta n = 0.05$ and $\Delta n = -0.05$, respectively. $\lambda = 1550$ nm. (c), (d) propagation of the same surface PLSs in the real (lossy) plasmonic lattices.

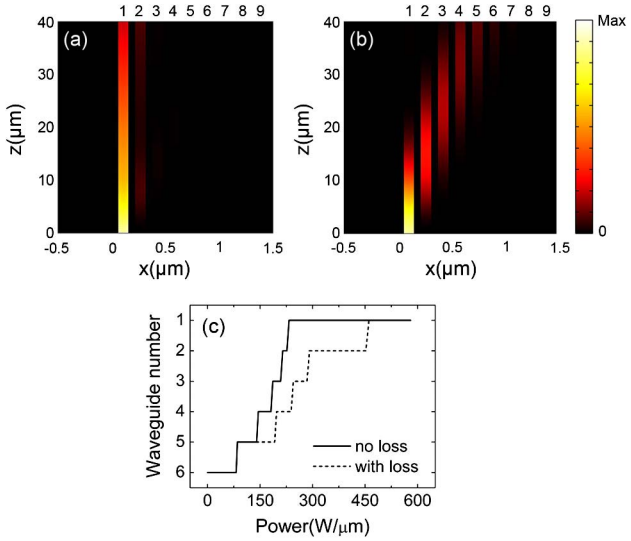

Fig. 4. (Color online) Nonlinear propagation of lossy SPP beams using single-waveguide excitation with input power (a) 360 W/μm and (b) 16 W/μm. $\lambda = 1550$ nm. (c) The output position of SPP beams versus input power, for a plasmonic lattice with length of 50 μm.

that at an input power of 360 W/μm, most of light remains within the first waveguide even after a distance of 40 μm [see Fig. 4(a)], indicating the formation of surface PLSs at this power level. As the input power decreases, linear diffraction gradually dominates, resulting in a significant shifting of the SPP beam toward the depth of the lattice [see Fig. 4(b)]. Thus, one could precisely select the output position of light through the control of the input power. Figure 4(c) shows the dependence of the location of the peak amplitude of light at the output facet of a plasmonic lattice, in both the ideal and lossy cases. Interestingly, the figure shows that in the lossy waveguide, switching the output position from the waveguide 6 to the waveguide 1 requires an incident power of 460 W/μm ($\Delta n \approx 0.11$), which is nearly twice the value of that in the lossless case. We finally mention that excitations from other waveguide (instead of the first waveguide) result in similar dependences of output position on input power.

In conclusion, we have studied the existence and properties as well as propagations of a new type of surface spatial solitons in a nonlinear semi-infinite plasmonic lattice, that is, surface PLSs. The impact of the lattice boundary on such surface states is elucidated. The boundary imposes a minimum power for the occurrence of surface PLSs, and the truncated lattice geometry leads to a significant modal compression.

This research was supported by the National Natural Science Foundation of China (Contract Nos. 10874119 and 61125503) and the Foundation for Development of Science and Technology of Shanghai (Grant Nos. 10JC1407200 and 11XD1402600).

References

1. D. N. Christodoulides, F. Lederer, and Y. Silberberg, Nature **424**, 817 (2003).
2. Y. Kivshar and G. Agrawal, *Optical Solitons: From Fibers to Photonic Crystals* (Academic, 2003).
3. Y. V. Kartashov, V. A. Vysloukh, and L. Torner, Prog. Opt. **52**, 63 (2009).
4. D. N. Christodoulides and R. I. Joseph, Opt. Lett. **13**, 794 (1988).
5. F. Lederer, G. I. Stegeman, D. N. Christodoulides, G. Assanto, M. Segev, and Y. Silberberg, Phys. Rep. **463**, 1 (2008).
6. K. G. Makris, S. Suntsov, D. N. Christodoulides, G. I. Stegeman, and A. Hache, Opt. Lett. **30**, 2466 (2005).
7. Y. V. Kartashov, V. A. Vysloukh, and L. Torner, Phys. Rev. Lett. **96**, 073901 (2006).
8. C. R. Rosberg, D. N. Neshev, W. Krolikowski, A. Mitchell, R. A. Vicencio, M. I. Molina, and Y. S. Kivshar, Phys. Rev. Lett. **97**, 083901 (2006).
9. Y. Liu, G. Bartal, D. A. Genov, and X. Zhang, Phys. Rev. Lett. **99**, 153901 (2007).
10. F. Ye, D. Mihalache, B. Hu, and N. C. Panoiu, Phys. Rev. Lett. **104**, 106802 (2010).
11. F. Ye, D. Mihalache, B. Hu, and N. C. Panoiu, Opt. Lett. **36**, 1179 (2011).
12. Y. Kou, F. Ye, and X. Chen, Phys. Rev. A **84**, 033855 (2011).
13. P. B. Johnson and R. W. Christy, Phys. Rev. B **6**, 4370 (1972).
14. M. Mitchell, M. Segev, T. H. Coskun, and D. N. Christodoulides, Phys. Rev. Lett. **79**, 4990 (1997).
15. J. Tian, S. Yu, W. Yan, and M. Qiu, Appl. Phys. Lett. **95**, 013504 (2009).
16. J. Wen, S. Romanov, and U. Peschel, Opt. Express **17**, 5925 (2009).